SCANNING VOL. 9999, 1–9 (2016)

Study of SEM Preparation Artefacts With Correlative Microscopy: Cell Shrinkage of Adherent Cells by HMDS-Drying

Alisa Katsen-Globa,[1] Norbert Puetz,[2] Michael M. Gepp,[1] Julia C. Neubauer,[1] and Heiko Zimmermann[1,3]

[1]Department for Cryo- and Stem Cell Technology, Fraunhofer Institute for Biomedical Engineering, Sulzbach, Germany
[2]Chair of Anatomy, Saarland University, Homburg, Germany
[3]Chair of Molecular and Cellular Biotechnology, Saarland University, Saarbrücken, Germany

Summary: One of the often reported artefacts during cell preparation to scanning electron microscopy (SEM) is the shrinkage of cellular objects, that mostly occurs at a certain time-dependent stage of cell drying. Various methods of drying for SEM, such as critical point drying, freeze–drying, as well as hexamethyldisilazane (HMDS)-drying, were usually used. The latter becomes popular since it is a low cost and fast method. However, the correlation of drying duration and real shrinkage of objects was not investigated yet. In this paper, cell shrinkage at each stage of preparation for SEM was studied. We introduce a shrinkage coefficient using correlative light microscopy (LM) and SEM of the same human mesenchymal stem cells (hMSCs). The influence of HMDS-drying duration on the cell shrinkage is shown: the longer drying duration, the more shrinkage is observed. Furthermore, it was demonstrated that cell shrinkage is inversely proportional to cultivation time: the longer cultivation time, the more cell spreading area and the less cell shrinkage. Our results can be applicable for an exact SEM quantification of cell size and determination of cell spreading area in engineering of artificial cellular environments using biomaterials. SCANNING 9999:1–9, 2016. © 2016 Wiley Periodicals, Inc.

Key words: light microscopy (LM), scanning electron microscopy (SEM), cell shrinkage, cell spreading area, hexamethyldisilazane (HMDS)

Conflicts of interest: None.

Address for reprints: Heiko Zimmermann, Department for Cryo- and Stem Cell Technology, Fraunhofer IBMT, Joseph-von-Fraunhofer-Weg 1, 66280 Sulzbach, Germany.
E-mail: heiko.zimmermann@ibmt.fraunhofer.de

Received 4 November 2015; Accepted with revision 5 February 2016

DOI: 10.1002/sca.21310
Published online XX Month Year in Wiley Online Library (wileyonlinelibrary.com).

Introduction

Scanning electron microscopy (SEM) has become increasingly important in cell biology—not only as a method for investigation of the surface topography of biological objects, but also as a tool for recognition of these objects with subsequent quantitative processing. Among other applications, it is of great importance to study the cell behavior on the biomedical materials (Curtis, 2001). Such research should focus on different cellular characteristics including cell proliferation, migration, attachment, and spreading on the engineered substrate. By screening of the new biomaterials cell spreading area can be performed and quantified with various methods including SEM (Richards *et al.*, ’97; Owen *et al.*, 2005; Katsen-Globa *et al.*, 2009). However, the precise determination of real cell size as well as cell area needs an artefact-free SEM-preparation.

After the implementation of SEM in biology, efforts of many researchers were directed on adequate preservation of native structures of biological objects with the minimal loss of their properties. Standard preparation for SEM includes pre-fixative treatment, fixation, and dehydration, as well as drying and following coating with the electro-conductive layer (Boyde, ’80; Brunk *et al.*, ’81). Each stage of the preparation can damage the specimen at a certain grade and might cause artefacts. It was concluded that especially dehydration and drying are prone to produce artefacts (Gusnard and Kirschner, ’77; Lytton *et al.*, ’79; Boyde and Maconnachie, ’80, ’81; Brunk *et al.*, ’81). For dehydration of fixed biological objects the water was first substituted with organic solvents such as ethanol, acetone, Freons, such as Freon 12 and Freon 113 (Boyde and Vesely, ’72; Boyde, ’80; Boyde and Maconnachie, ’80, ’81), and then dried. For drying, various methods were applied whereas the most popular were critical point drying (CPD), freeze–drying, and hexamethyldisilazane (HMDS)-drying (Boyde and Vesely, ’72; Boyde *et al.*, ’72, ’81; Billings-Gagliardi *et al.*, ’78; Boyde, ’80; Brunk *et al.*, ’81; Draenert and

Draenert, '82; Nation, '83; Nordestgaard and Rostgaard, '85; Dekker *et al*., '91; Bray *et al*., '93; Braet *et al*., '97; Fratesi *et al*., 2004; Jahn *et al*., 2007; Wisse *et al*., 2010; Lee and Chow, 2011; Hazrin-Chong and Manefield, 2012). Comparative efficiency of these methods was discussed in numerous publications revealing that the most frequent artefacts of all methods are formation of ruptures, disappearance of intercellular contacts, and particularly, cell shrinkage of the original volume up to 50% (Schneider, '76; Gusnard and Kirschner, '77; Billings-Gagliardi *et al*., '78; Lytton *et al*., '79; Boyde, '80; Boyde and Maconnachie, '80, '81; Wollweber *et al*., '81; Nordestgaard and Rostgaard, '85). In particular, the following aspects have been extensively studied and compared by CPD and freeze–drying, and the most general agreement that freeze–drying is a technique introducing less shrinkage than CPD, and preserving similar or better fine cellular surface morphology (Boyde and Vesely, '72; Boyde *et al*., '72; Billings-Gagliardi *et al*., '78; Boyde and Maconnachie, '79, '81; Brunk *et al*., '81). However, also freeze-drying can cause SEM artefacts due to ice crystal formation (Boyde and Maconnachie, '81; Draenert and Draenert, '82; Nordestgaard and Rostgaard, '85). Although shrinkage caused by HMDS was not intensively studied, it was noted to be comparable with CPD results (Dekker *et al*., '91; Braet *et al*., '97; Jahn *et al*., 2007).

In the above mentioned studies, the assessment of cell shrinkage was mainly based on suspended cells or pieces of tissue. In contrast, cell ruptures and loss of cellular contacts were mostly observed and described for adherent cultured cells (Schroeter *et al*., '84). However, a precise investigation of these artefacts was marginally performed. The damage of the cytoskeleton structures can be a reason of such artefacts (Wollweber *et al*., '81; Schroeter *et al*., '84), and cause the cell shrinkage with following change of cell volume and/or cell area. Taking into account cell shrinkage at the calculation of the cell spreading area will better reflect the biological reality.

Some years ago, we developed a new SEM-based method for automatic analysis of cell attachment and spreading area (Katsen-Globa *et al*., 2009). In this study the shrinkage of cells caused by preparation for SEM was not considered. Later, applying the developed method for evaluation of cryopreserved adherent cells, we took into account this artefact by introducing the area shrinkage coefficient (Katsen-Globa *et al*., 2014). In this work we have dried the samples 10 min in HMDS, according to the recommended time in literature (Dekker *et al*., '91).

In the present study, we have investigated in detail the changes of cell spreading area at different stages of SEM preparation. For exact calculation of cell shrinkage, correlative light microscopy (LM), and SEM of the same cell objects were applied. The identification of the same cells in both, LM and SEM was performed using the commercial culture dishes with grids (Katsen-Globa *et al*., 2014; Madela *et al*., 2014). Studying hMSCs we have investigated the dependence of drying duration and the influence of cell cultivation time/spreading on cell shrinkage. The areas of the same cells were measured by analyzing LM-, and SEM-images (automatically or manually) at each stage of SEM preparation.

Materials and Methods

Cell Cultivation

Umbilical cord hMSCs (PromoCell GmbH, Heidelberg, Germany) were inoculated with a density of 5×10^3 cells/cm^2 and cultivated 2, 4, and 24 h according to manufacturer's protocol in 35 mm μ-dishes with grid (ibidi GmbH, Martinsried, Germany). For each time point, three dishes were used and each experiment was repeated three times (n = 3).

For comparison CPD-, and HMDS-drying, L929 mouse fibroblasts were cultivated at 37°C, 5% CO_2/95% air in Dulbecco's modified growth medium with 10% bovine serum and antibiotics. The cells were detached with trypsin/EDTA and used as suspension for following SEM preparation. All reagents were purchased from Life Technologies GmbH (Darmstadt, Germany).

Light Microscopy (LM)

To estimate cell shrinkage during SEM preparation, the same cells were studied and photographed under the liquid layer of culture medium using phase contrast microscopy (Eclipse TS100, Nikon GmbH, Duesseldorf, Germany). The same observed field of view was imaged before and after fixation, as well as after treatment with osmium tetroxide, tannic acid, and uranyl acetate (see Fig. 1). At least four images per approach/dish were taken in all samples.

Scanning Electron Microscopy (SEM)

To evaluate cell morphology and spreading, the adherent hMSCs, cultivated in the μ-dishes, were prepared to SEM as previously described (Katsen *et al*., '92) and modified (Katsen *et al*., '98). Briefly, the samples were washed with PBS, fixed overnight in 2% glutaraldehyde in 0.1 M sodium cacodylate buffer (osmolarity 330 mOsm) and post-fixed in 2% osmium tetroxide in sodium cacodylate buffer, then treated with 1% tannic acid and 1% uranyl acetate, both in water. After dehydration in increasing concentrations of ethanol (10%, 20%, 30%, 40%, 50%, 60%, 70%, 80%, 90%, and

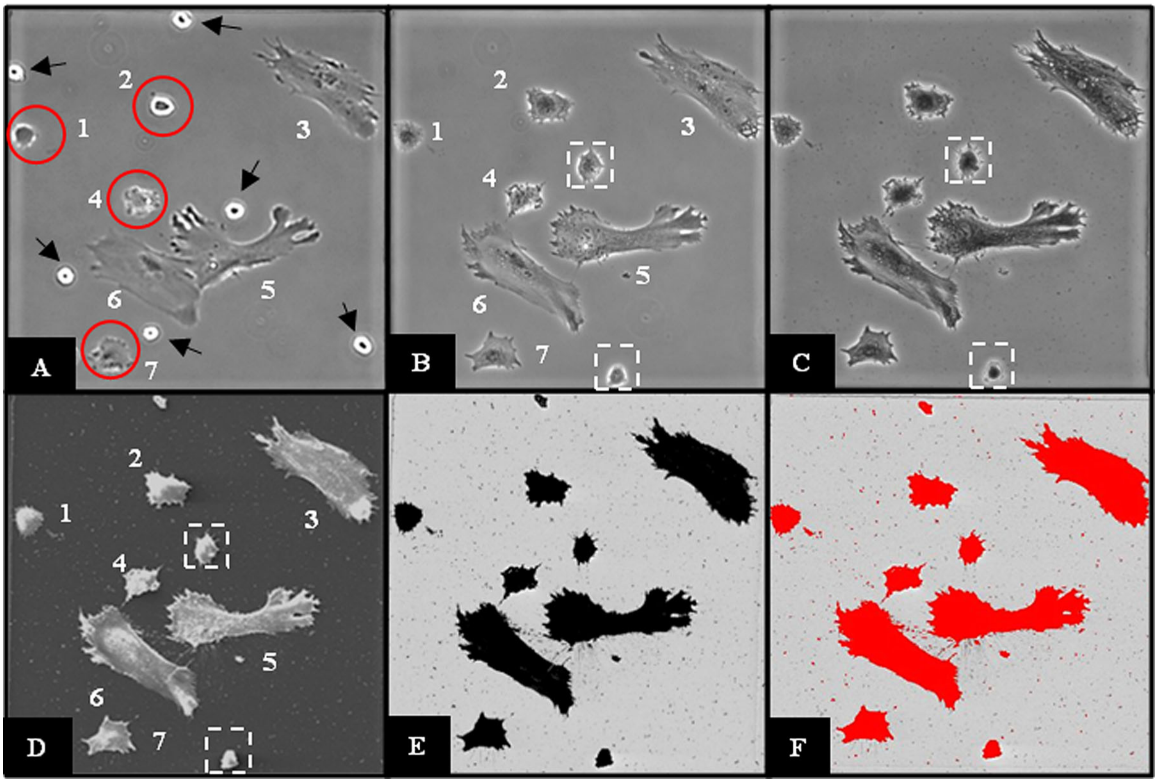

Fig 1. Representative images of combined light microscopy (LM), and scanning electron microscopy (SEM) of the same hMSCs cultivated in dishes with grids. LM-images present living hMSCs (A), the same cells after fixation (B), and the same ones after treatment with tannic acid and heavy metals (C). SEM-images showing the same field of view, performed in secondary electron (SE) mode (D), inverted image in backscattered electron (BSE) mode (E), and after threshold segmentation, performed in ImageJ program (F) and suitable for automatic measurement of cell area.

100%, 3 min in each concentration), the samples were dried for 3 min in mixing 1:1 100%-ethanol and hexamethyldisilazane (HMDS, Sigma–Aldrich GmbH, Taufkirchen, Germany) with subsequent 3 min drying in pure HMDS.

Three time durations of HMDS-drying were compared: 3 min, 5 min and previously proved 10 min (Katsen-Globa *et al.*, 2014). About 300 cells in each group were analyzed in this study.

In order to compare the cell surface preservation by CPD and HMDS-drying, we have used a cell suspension of L929 cells. The cells were placed in Millicell culture inserts (12 mm in diameter, PXPO1250, Millipore), fixed and prepared for SEM as above described.

All dried samples were immediately coated with carbon in SCD-030 coating device (Balzers, Lichtenstein), then studied and imaged in the field emission scanning electron microscope, Phillips, FESEM XL30 (FEI, Eindhofen, Netherlands). The same cells previously photographed in LM were identified and imaged in secondary electron (SE)-, and backscattered electron (BSE)-modes. For SE imaging, an accelerating voltage of 5 and 10 kV was used. Cell spreading areas were studied with backscattered electron (BSE) modes at 10 kV accelerating voltage, and 10 mm working distance for all images.

Image Analysis and Determination of Changes of Cell Area

Cell spreading area was measured using inverted BSE-images with high contrast as previously developed (Katsen-Globa *et al.*, 2009) and recently modified and described (Katsen-Globa *et al.*, 2014). BSE-images were acquired in SEM by 150× magnification. We have measured the cell area both, automatically and manually, using online available ImageJ software (NIH, Bethesda, MD). Briefly, the cell areas were marked automatically by *threshold segmentation* or manually using *freehand selection*, and then automatically measured using *analyze tools* of the ImageJ program.

The cell spreading area was measured using LM-, and SEM BSE- images of the same cells (see Fig. 1 and Table I). Shrinkage coefficients were calculated: (i) for fixation—by dividing of living cell area (LM, Fig. 1(A)) to cell area after fixation with glutaraldehyde (LM, Fig. 1(B)); (ii) for post-fixation treatment—by dividing of cell area of fixed cell (LM, Fig. 1(B)) to cell area after treatment with tannic acid and heavy metals (LM, Fig. 1(C)); and (iii) for SEM preparation—by dividing of cell area after tannic acid and heavy metals treatment (LM, Fig. 1(C)) to cell area measured in BSE (SEM, Fig. 1(E and F)).

TABLE I Representative data of cell area and shrinkage coefficient at all stages of SEM-preparation

Cell	Cell area (μm²)				Shrinkage coefficient		
	LM live	LM after fixation	LM after treatment	SEM	Fixation	Treatment	SEM
1	528	949	935	865	0.56	1.01	1.08
2	695	1670	1683	1498	0.42	0.99	1.12
3	6669	7884	7891	7342	0.85	1	1.07
4	1132	1346	1354	1039	0.84	0.99	1.3
5	7439	7701	7568	6984	0.97	1.02	1.08
6	7534	7880	7877	7089	0.96	1	1.11
7	1591	1699	1692	1494	0.94	1	1.13
Mean value ± s.d.					0.79 ± 0.20	1.00 ± 0.01	1.13 ± 0.07

Spreading areas were calculated for cells, numbered as 1–7 in Figure 1.

Three experiments were carried out for only 3 min of HMDS-drying. The areas of more than 100 cells per approach were measured and more as 400 cells in total at each time point were processed.

Statistical Analysis

Statistical results are presented as mean value ± standard deviation (s.d.), evaluated with Student's *t*-test and considered significant by $p < 0.05$.

Results

Cell Shrinkage at Different Stages of SEM Preparation

For the first time, we have compared the cell shrinkage area during all steps of SEM-preparation performed with the same adherent cells (see Fig. 1). Various events at the different stages of SEM-preparation could be revealed. For example, some observed living cells were detached during live cell imaging, washing, and fixation (Fig. 1(A), cells marked with arrows). The time between live cell imaging and fixation took about 15 min. During this time, some cells, marked in Figure 1(A) with circles, spread, whereas other cells changed their position (compare cells 5 and 6 in Fig. 1(A and B)). Also, some cells have moved and attached during fixation (Fig. 1 (B, C and D, cells with dashed line), the cells, squared with dashed line). Due to enhanced contrast of the inverted BSE-images (Fig. 1(E)), automatic threshold segmentation enabled a valid detection and separation method for cell contours (Fig. 1(F)).

Representative calculations of cell spreading areas of the cells, numbered as 1–7 in Figure 1, as well as estimated cell shrinkage coefficients are presented in Table I. As illustrated, cell shrinkage coefficients decrease during fixation. In contrast, at the time of post-fixation with osmium tetroxide, treatment with tannic acid, and uranyl acetate, the areas of cells remain almost constant. Contrary, at the time of dehydration and HMDS-drying, shrinkage of cell area increases.

We have measured the cell areas of 126 cells (data not shown) and derived a shrinkage coefficient due to fixation of 0.84 ± 0.18, while the shrinkage coefficient after heavy metals and tannic acid treatment was 1.01 ± 0.04.

Preservation of Cell Surface by HMDS-Drying

In this work, the surface preservation after CPD (Fig. 2(A)) and HMDS-drying (Fig. 2(B)) have been compared. Both methods showed excellent preserved microvilli of suspended L929 mouse fibroblasts, the typical cell surface features of these cells.

Also, SEM SE-images of attached and spread hMSCs revealed good quality of HMDS-drying (Fig. 3). After 2 h cultivation, round cells covered with numerous long microvilli were observed (Fig. 3(A and B)). Simultaneously, a not well-spread cell with numerous

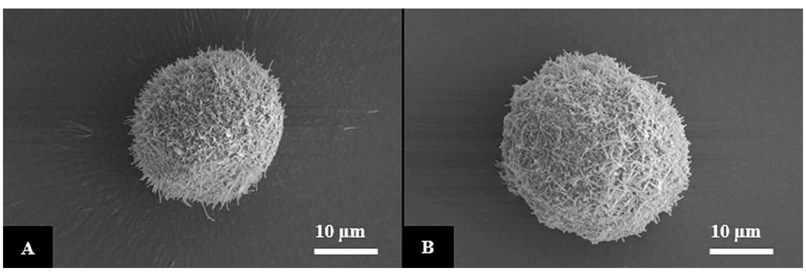

Fig 2. Representative SE-images of suspended L929 cells, dried with CPD (A) and HMDS (B).

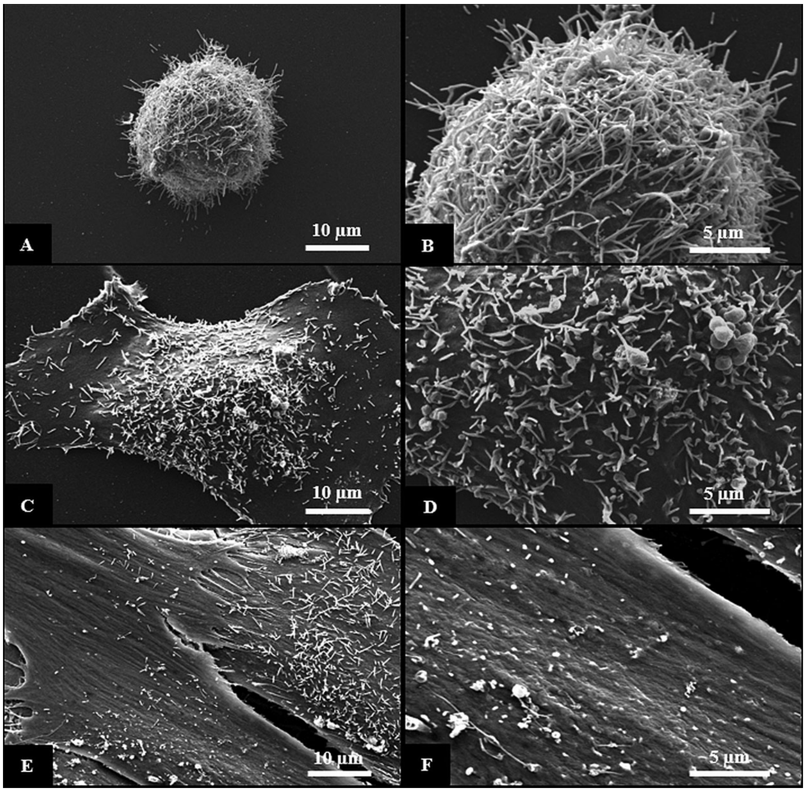

Fig 3. Representative secondary electron SEM-images of surface features HMDS-dried adherent hMSCs. (A) a round, non-spread cell after 2 h cultivation; (B) high magnification of the cell presented in A. C: non-well spread cell after 2 h cultivation; (D) high magnification of the cell presented in C. (E) flat well-spread cell after 24 h cultivation; (F) high magnification of the cell (left) presented in E.

microvilli, shorter compared to the round cells, and with some surface vesicles were presented (Fig. 3(C and D)). After 24 h cultivation, mostly flat cells covered with singular short microvilli and some vesicles were recognized (Fig. 3(E and F)).

Effect of HMDS-Drying Duration

We have studied the effect of HMDS-drying duration on the cell shrinkage. To estimate cell shrinkage, the areas of cells in BSE-images (such as in Fig. 1E) have been measured. About 300 cells in each group were analyzed, and the differences between mean values of cell shrinkage were statistical significant ($p < 0.05$). As seen in Figure 4, cell shrinkage is proportional to the duration of HMDS-drying: the longer the drying duration, the higher the cell shrinkage. As 3 min HMDS-drying caused the smallest cell shrinkage, all other experiments have been carried out according to this protocol.

Effect of Cell Spreading on Cell Shrinkage

According to previously described data, further three experiments were performed with 3-min HMDS-drying and different cell cultivation time as described in Materials and Methods. To estimate shrinkage coefficient, we have analyzed the cell areas after the treatment with heavy metals in comparison to the cell area based on SEM-images. Quantification of cell area has indicated that cell area increases with the time of cultivation (Fig. 5).

The results of cell shrinkage in three separate experiments are presented in Table II and summarized as diagram in Figure 6. For each group, the areas of more

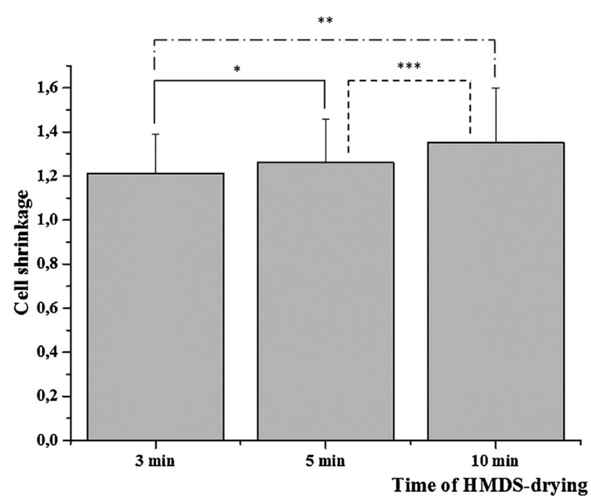

Fig 4. Effect of HMDS-drying duration on the cell shrinkage. The differences between groups (*, **, and ***) were statistically significant ($p < 0.05$).

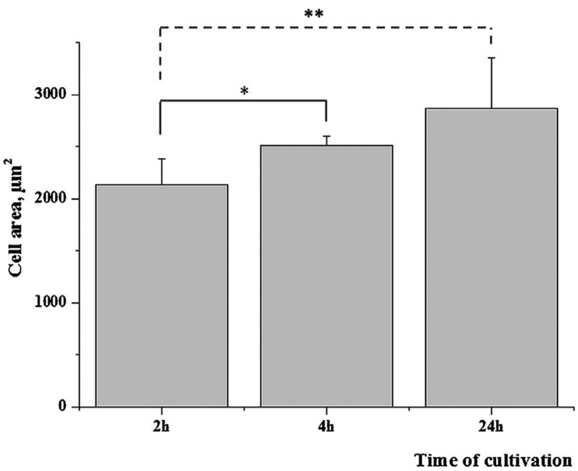

Fig 5. Effect of time of cultivation on the cell spreading. The differences between 2 h and 4 h (*), as well as 2 h and 24 h (**) were statistically significant ($p < 0.05$), the difference between 4 h and 24 h was not statistically significant ($p < 0.05$).

than 400 cells were measured and evaluated. Our results revealed that cell shrinkage has decreased with the time of cell cultivation, and the differences between the groups were statistical significant ($p < 0.05$).

Discussion

For the first time, we have studied the changes of areas of the same adherent hMSCs at different stages of SEM-preparation. In this investigation the duration of HMDS-drying and the time of cell cultivation were varied. We can summarize our results as follows.

Cell Surface Properties After HMDS-Drying Are Not Different From Ones After CPD

This part of study was performed with suspended L929 mouse fibroblasts and no differences between CPD and HMDS-drying were detected (compare Fig. 2 (A and B)).

Also, HMDS-drying of adherent hMSCs has revealed the excellent preservation of fine cell surface features (Fig. 3). The observed changes of number and length of microvilli (compare Fig. 3B with D and F) can be explained by various degrees of cell spreading on the substrate (Erickson and Trinkaus, '76).

Our results are in agreement with other studies that compared CPD and HMDS-drying by processing various biological objects, such as soft insect tissue (Nation, '83), rat trachea cilia (Bray *et al*., '93), liver endothelial cells (Braet *et al*., '97), as well as cervical cells (Jusman *et al*., 2014), and even biofilms (Fratesi *et al*., 2004). Our long-term experience with both, CPD and HMDS-drying of different kinds of fibroblasts, cardiomyocytes, hepatocytes, Langerhans islands, multicellular spheroids from stem cells, and others cells shows that HMDS does not concede on quality to CPD (Metzger et al., 2011; Heras-Bautista et al., 2014), the standard method of preparation for SEM. In comparison to CPD, HMDS-drying is a fast, simple and inexpensive method that requires any other special equipment except a laboratory fume hood (Dekker *et al*., '91; Braet *et al*., '97; Wisse *et al*., 2010; Lee and Chow, 2011; Jusman *et al*., 2014). HMDS-drying can be the method of choice in many applications, especially by simultaneous processing at the same time a large number of the samples that would be unacceptable for the relative small volume of standard CPD-device chambers.

Since the presented study continues recently published work concerning cryopreservation of adherent mesenchymal stem cells via SEM for vitality and recovery assessment of hMSCs (Katsen-Globa *et al*., 2014), HMDS-drying was not explicitly compared to established and described freeze–drying methods (Boyde and Wood, '69; Boyde and Vesely, '72; Boyde and Maconnachie, '81). Furthermore, ice crystal formation during cryopreservation may cause artefacts, such as holes in cell membranes or cell shrinkage, equal to freeze–drying artefacts. The identification of causative aspects for these artefacts, thus, is extremely difficult. Due to the excellent preservation of cell surface morphology, the used HMDS-drying finally serves as an acceptable alternative to other drying methods.

The Duration of HMDS-Drying Influences Cell Shrinkage: The Longer Drying Duration, the More Cell Shrinkage

Various drying durations are published and chosen according to the size of samples: 3 min for cell cultures (Jahn *et al*., 2007), 5 min for soft insect tissue (Nation,

TABLE II Shrinkage of cell areas caused of HMDS-drying, determined in three separate experiments

	2 h cultivation		4 h cultivation		24 h cultivation	
Experiment	Shrinkage	Cell number	Shrinkage	Cell number	Shrinkage	Cell number
1	1.25	139	1.25	113	1.16	139
2	1.31	115	1.26	164	1.15	147
3	1.23	207	1.17	174	1.14	141
Mean value ± s.d.	1.26 ± 0.03	461	1.23 ± 0.04	451	1.15 ± 0.01	427

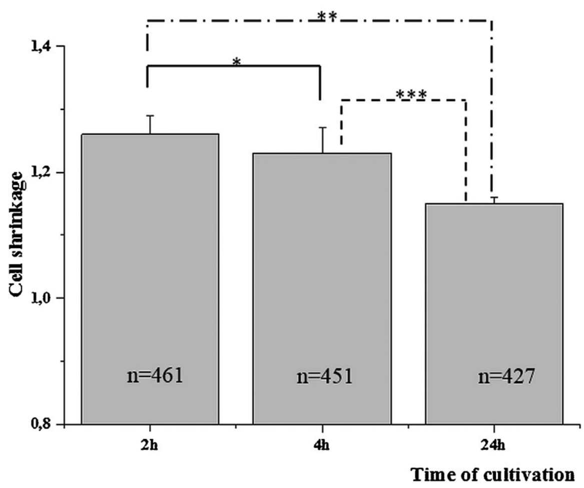

Fig 6. Effect of cultivation time on the cell shrinkage. The differences between 2 h and 4 h (*), as well as 2 h versus 24 h (**) and 4 h versus 24 h (***) were statistically significant ($p < 0.05$).

'83), 10 min for mucosal cells (Dekker *et al.*, '91) and liver tissue (Wisse *et al.*, 2010), and up to 30 min for 1–3 mm^3 blocks of different tissues (Bray *et al.*, '93). In our previous paper, we have dried hMSCs within alginate sponges for 10 min in HMDS (Katsen-Globa *et al.*, 2014). In the present study, we have also investigated hMSCs, but adherent and well-spread on plastic substrates. Our experiments revealed that drying for 3 min in HMDS was adequate in order to preserve cellular features. In general, this time must be verified and adopted for each specific type of cell or tissue. Longer time periods of about 30 min of HMDS-drying showed cell culture damages due to massive membrane disruptions (data not shown).

In fact, a valid differentiation of cell shrinkage caused by either HMDS-drying or ethanol dehydration is not possible. Dehydration studies of erythrocytes and hepatocytes (Gusnard and Kirschner, '77), mouse embryo limbs (Boyde and Maconnachie, '79 and 1981), and mouse liver (Boyde and Maconnachie, '83) revealed the highest shrinkage and distortion of cells/tissue due to solvent evaporation during dehydration process.

Boyde and Maconnachie ('81) have shown that: (i) dehydration in 30% and 50% ethanol causes swelling with disruption of the tissue and (ii) dehydration between 70% and 80 % ethanol causes the greatest shrinking. To minimize swelling the authors proposed addition of Ca^{2+} cations prior or during dehydration (Boyde and Maconnachie, '79, '81), to minimize shrinkage—starting of dehydration in 70% or even 100% ethanol (Boyde and Maconnachie, '81), or treatment with different salts (Boyde and Maconnachie, '80). Substitution of 100% ethanol with low surface tension volatile solvents such as Freon 113 or diethyl ether before CPD or freezing the samples in Freon 12 before transfer in liquid nitrogen with following freeze–drying can also minimize shrinkage artefacts (Boyde and Maconnachie, '81).

To reduce preparation shrinkage, we are using more than 20 years the method including treatment of fixed with glutaraldehyde and osmium tetroxide cells with tannic acid and uranyl acetate, proposed first by Wollweber *et al.* ('81) and later modified (Katsen *et al.*, '92, '98). This method with subsequent dehydration in increased ethanol gradients with short incubation time (3 min) can also minimize cell shrinkage. This kind of dehydration with following drying of low tension volatile non-polar solvent HMDS reveals adequate results, as presented here. The usage of acetone instead of ethanol was rejected due to more shrinkage by dehydration and because plastic dishes with grids, made from polystyrene, are not chemical resistant to acetone. As dried specimens are highly hygroscopic, its subsequent transfer in the carbon coating device must be quick or both processes have to be made in the same vacuum chamber (Boyde and Wood, '69). In consequence, we reject LM to measure the cell spreading area of dehydrated with ethanol samples that need about 15 min for imaging and can be a reason of rehydration of materials.

Finally, dehydration time was the same for all experiences. In consequence, we can claim that drying duration influences cell shrinkage.

Cell Changes Occurred at Each Stage of SEM Preparation

During live cell imaging, medium change and fixation, cells can detached from the substrate, while cells already attached to the surface, can move and spread (compare Fig. 1(A and B)). This effect can be explained with relative long (15 min) duration of live cell microscopy/imaging. The process of fixation with glutaraldehyde does not happen immediately and takes some time that is enough for cell moving and following spreading. As consequence, cell spreading area has increased and, respectively, cell shrinkage coefficient has decreased. Some authors described also shrinkage artefacts caused by fixation using hyperosmotic fixator (Loqman *et al.*, 2010). In our study, we have used isosmotic fixative solution in order to avoid such artefacts. It should be possible to elude the changes of cell area described above, if the fixation is made immediately after cultivation and without live cell microscopy.

The cell shrinkage coefficient after treatment with tannic acid and heavy metals changed marginally and can be neglected. Applied chemical treatment of specimens was proposed exactly for stabilizing of the cytoskeleton and avoiding of cell shrinkage (Wollweber *et al.*, '81; Schroeter *et al.*, '84; Katsen *et al.*, '92, '98). In this paper we have quantitatively confirmed this assumption.

To measure the cell spreading area, various LM methods such as confocal microscopy, IRM, and TIRFM

(Curtis, 2001) could be applied. However, these methods were created and used mostly for glass substrates, but are difficult for imaging of cells on plastic dishes with grids. In our case, using of chosen phase-contrast LM method for quick recognition of cell contours with following determination of cell spreading area of wet cells was adequate.

Shrinkage Coefficient Is Dependent From Degree of Cell Spreading: The More Cell Spreading, the Less Its Shrinkage

This speculation refers to cytoskeleton and cell-substrate contacts. These contacts, mediated by cytoskeleton proteins, are involved in the attachment and spreading of cells (Gumbiner, '96) and depend on the cultivation time (Anselme and Bigerelle, 2006): the longer the cultivation time, the more the cell spreading (see Fig. 5) and the stronger cell-substrate contacts during cell spreading. On the one hand, the increased number of such contacts does not allow objects, such as cells, to contract. As a result, the shrinkage coefficient, especially by short drying (3 min), decreases (see Table II and Fig. 6). On the other hand, the existence of such anchorages with suppressed cell shrinkage can explain the formation of ruptures in cellular membranes during drying. Partially, these artefacts can be avoided by applying the treatment of cells with tannic acid and heavy metals in order to stabilize the cytoskeleton. Another possibility is the coating of the substrate with an elastic support, such as extracellular matrix (ECM) or ECM components (such as collagen or fibronectin): the cells may contract together with ECM, and membrane ruptures will not appear. Our experience with the cardiomyocytes cultivated on the plastic substrate covered with ECM as well as studying hMSCs within alginate-collagen sponges, confirms this speculation (data not shown).

Conclusions

Comparison With Cell Volume Shrinkage

In this study we have measured the cell area of spread cells. Actually, we cannot compare our results with previously described cell volume shrinkage, since this data based mostly on suspended cells or tissue (Schneider, '76; Gusnard and Kirschner, '77; Billings-Gagliardi *et al.*, '78; Lytton *et al.*, '79; Boyde, '80; Boyde et al., '81; Wollweber et al., '81; Nordestgaard and Rostgaard, '85; Jahn et al., 2007). The measuring and quantification of the cell volume of adherent cells is more difficult: here, it can be helpful only to study sagittal serial sections performed with conventional transmission electron microscopy or block-face SEM (Denk and Horstmann, 2004) and subsequent volume reconstitution. Indirectly, considering studied hMSCs are well-spread on a substratum and their height is very low (about 0.5 μm), the contribution of this parameter to the total amount of cell volume can be insignificant. In this case we can speculate about minor cell shrinkage during HMDS-drying of well-spread cells.

Use of Shrinkage Coefficient in SEM Investigation

Cell-substrate interaction such as cell adhesion to substrate with following spreading is a key aspect of cell-biomaterial research (Curtis, 2001). To compare cell reaction on various materials, the adhesion and spreading of single cells must be quantified. High-resolution SEM was applied for measuring of either focal adhesions (Owen *et al.*, 2005) or the whole cell area quantification (Richards *et al.*, '97; Katsen-Globa *et al.*, 2009). However, in the above mentioned studies, shrinkage of cells during SEM-preparation was not taken into account. Certainly, this is very important, when the artefacts caused by SEM-preparation, are similar to that one caused by observed effects such as cell dehydration during cryopreservation. SEM can be a useful tool for estimation of cell membrane response to cryodamage (Ragoonanan *et al.*, 2013; Katsen-Globa *et al.*, 2014). During slow-freezing, shrinkage of water occurs, which can lead to osmotic shrinkage with following cell area/volume reduction and even cell death (Ragoonanan *et al.*, 2013; Katsen-Globa *et al.*, 2014). To differentiate these two kinds of shrinkage occurred in freezing process and SEM-preparation, the shrinkage coefficient can be useful for exact quantification of the cell area (Katsen-Globa *et al.*, 2014).

Another aspect is the knowledge of real cell size by SEM-investigation. It can be widely used for SEM-identification of different cell types (Lytton *et al.*, '79), such as blood cells, hepatic cells, etc.

Acknowledgments

The authors would like to thank Dr. F. Volke, Fraunhofer IBMT, for critical proof-reading and helpful discussion.

References

Anselme K, Bigerelle M. 2006. Modelling approach in cell/material interactions studies. Biomaterials 27:1187–1199.

Billings-Gagliardi S, Pockwinse SM, Schneider GB. 1978. Morphological changes in isolated lymphocytes during preparation for SEM: freeze-drying versus critical-point drying. Am J Anat 152:383–389.

Boyde A. 1980. Review of basic preparation techniques for biological scanning electron microscopy. In: Brederoo P, de Priester W, editors. Electron microscopy. The Hague: 7th Eur Leiden: Congress Electron Microscopy Foundation; 2. p 768–777.

Boyde A, Franc F, Maconnachie E. 1981. Measurements of critical point shrinkage of glutaraldehyde fixed mouse liver. Scanning 4:69–82.

Boyde A, Maconnachie E. 1979. Volume changes during preparation of mouse embryonic tissue for SEM. Scanning 2:149–163.

Boyde A, Maconnachie E. 1980. Treatment with litium salts reduces ethanol dehydration shrinkage of glutaraldehyde fixed tissue. Histochemistry 66:181–187.

Boyde A, Maconnachie E. 1981. Morphological correlations with dimensional changes during SEM specimen preparation. Scanning Electron Microsc 4:27–34.

Boyde A, Maconnachie E. 1983. Not quite critical point drying. In: Revel JP, Barnard T, Haggis GH, editors. The science of biological specimen preparation for microscopy and microanalysis. Chicago, IL: SEM Inc., AMF O'Hare. p 71–75.

Boyde A, Vesely P. 1972. Comparison of fixation and drying procedures for preparation of some cultured cell lines for examination in the SEM. In: Johari O, Corvin I, editors. Scanning electron microscopy. Chicago, IL: IIT Research Institute. p 265–272.

Boyde A, Weiss RA, Vesely P. 1972. Scanning electron microscopy of cells in culture. Exp Cell Res 71:313–324.

Boyde A, Wood C. 1969. Preparation of animal tissues for surface scanning electron microscopy. J Microsc 90:221–249.

Braet F, De Zanger R, Wisse E. 1997. Drying cells for SEM, AFM, and TEM by hexamethyldisilazane: a study on hepatic endothelial cells. J Microsc 186:84–87.

Bray DF, Bagu J, Koegler P. 1993. Comparison of hexamethyldisilazane (HMDS), peldri 11, and critical-point drying methods for scanning electron microscopy of biological specimens. Microsc Res Tech 26:489–495.

Brunk U, Collins VP, Arro E. 1981. The fixation, dehydration, drying and coating of cultured cells of SEM. J Microsc 123:121–131.

Curtis AS. 2001. Cell reactions with biomaterials: the microscopies. Eur Cell Mater 1:59–65.

Dekker NP, Lammel CJ, Brooks GF. 1991. Scanning electron microscopy of piliated Neisseria Gonorrhoeae processed with hexamethyldisilazane. J Electron Microsc Tech 19:461–467.

Denk W, Horstmann H. 2004. Serial block-face scanning electron microscopy to reconstruct three-dimensional tissue nanostructure. PLoS Biol 2:e329.

Draenert Y, Draenert K. 1982. Ice crystal damage in freeze-dried articular cartilage studied by scanning electron microscopy. Scan Electron Microsc Pt4:1799–1804.

Erickson CA, Trinkaus JP. 1976. Microvilli and blebs as a source of reserve surface membrane during cell spreading. Exp Cell Res 99:375–384.

Fratesi S, Lynch F, Kirkland BL, et al. 2004. Effects of SEM preparation techniques on the appearance of bacteria and biofilms in the Carter Sandstone. J Sediment Res 74:858–867.

Gumbiner BM. 1996. Cell adhesion: the molecular basis of tissue architecture and morphogenesis. Cell 84:345–357.

Gusnard D, Kirschner RH. 1977. Cell and organelle shrinkage during preparation for scanning electron microscopy: effects of fixation, dehydration and critical point drying. J Microsc 110:51–57.

Hazrin-Chong NH, Manefield M. 2012. An alternative SEM drying method using hexamethyldisilazane (HMDS) for microbial cell attachment studies on sub-bituminous coal. J Microbiol Methods 90:96–99.

Heras-Bautista CO, Katsen-Globa A, Schloerer NE, et al. 2014. The influence of physiological matrix conditions on permanent culture of induced pluripotent stem cell-derived cardiomyocytes. Biomaterials 35:7374–7385.

Jahn K, Barton D, Braet F. 2007. Correlative fluorescence- and scanning, transmission electron microscopy for biomolecular investigation. In: Méndez-Vilas A, Dı́az J, editors. Modern research and educational topics in microscopy. Badajoz, Spain: FORMATEX. p 203–2011.

Jusman Y, Ng SC, Osman NAA. 2014. Investigation of CPD and HMDS sample preparation techniques for cervical cells in developing computer-aided screening system based on FE-SEM/EDX. Sci World J 2014. Article ID 289817.

Katsen AD, Tregubova NA, Andrushkevich VV, et al. 1992. Identification and study of the same cell in monolayer culture by different methods of light microscopy, scanning and transmission electron microscopy. Application for cryodamaged cells. Scanning 14:225–230.

Katsen AD, Vollmar B, Mestres-Ventura P, et al. 1998. Cell surface and nuclear changes during TNF-α-induced apoptosis in WEHI-164 murine fibrosarcoma cells. A correlative light-, scanning-, and transmission electron microscopical study. Virchows Arch 433:75–83.

Katsen-Globa A, Peter L, Zoellner S, et al. 2009. A novel approach for automated analysis of cell attachment and spreading based on backscattered electron imaging by scanning electron microscopy. Materials 2:1402–1416.

Katsen-Globa A, Meiser I, Petrenko YA, et al. 2014. Towards ready-to-use 3-D scaffolds for regenerative medicine: adhesion-based cryopreservation of human mesenchymal stem cells attached and spread within alginate-gelatin cryogel scaffolds. J Mater Sci Mater Med 25:857–871.

Lee JTY, Chow KL. 2011. SEM sample preparation for cells on 3D scaffolds by freeze-drying and HMDS. Scanning 33:1–14.

Loqman MY, Bush PG, Farquharson C, Hail AC. 2010. A cell shrinkage artefact in growth plate chondrocytes with common fixative solutions: importance of fixative osmolarity for maintaining morphology. Eur Cell Mater 19:214–227.

Lytton DG, Yuen E, Rickard KA. 1979. Scanning electron and light microscope correlation of individual human bone marrow cells before and after culture in nutrient agar. J Microsc 115:35–49.

Madela K, Banhart S, Zimmermann A, et al. 2014. A simple procedure to analyze position of interest in infectious cell cultures by correlative light and electron microscopy. In: Müller-Reichert T, Verkade P, editors. Methods in cell biology, vol. 124. Burlington: Academic Press. p 93–110.

Metzger W, Sossong D, Bächle A, et al. 2011. The liquid overlay technique is the key to formation of co-culture spheroids consisting of primary osteoblasts, fibroblasts and endothelial cells. Cytotherapy 13:1000–1012.

Nation JL. 1983. A new method using hexamethyldisilazane for preparation of soft insect tissues for scanning electron microscopy. Stain Technol 58:347–351.

Nordestgaard BG, Rostgaard J. 1985. Critical-point drying versus freeze-drying for scanning electron microscopy: a quantitative and qualitative study on isolated hepatocytes. J Microsc 137:189–207.

Owen GR, Meredith DO, ap Gwynn I, et al. 2005. Focal adhesion quantification—a new assay of material biocompatibility? Rev Eur Cell Mater 9:85–96.

Schneider GB. 1976. The effects of preparative procedures for scanning electron microscopy on the size of isolated lymphocytes. Am J Anat 146:93–100.

Schroeter D, Spiess E, Paweletz N, et al. 1984. A procedure for rupture-free preparation of confluently grown monolayer cells for scanning electron microscopy. J Electron Miscrosc Technol 1:219–225.

Ragoonanan V, Less R, Aksan A. 2013. Response of the cell membrane-cytoskeleton complex to osmotic and freeze/thaw stresses. Part 2: the link between the state of the membrane-cytoskeleton complex and the cellular damage. Cryobiology 66:96–104.

Richards RG, Owen GR, Rahn BA, et al. 1997. A quantitative method of measuring cell-substrate adhesion areas. Cells Mater 7:15–30.

Wisse E, Braet F, Duimel H, et al. 2010. Fixation methods for electron microscopy of human and other liver. World J Gastroenterol 16:2851–2866.

Wollweber L, Stracke R, Gothe U. 1981. The use of a simple method to avoid cell shrinkage during SEM preparation. J Microsc 121:185–189.